Series-fed Dipole Array for Near-field RFID Application

Yi Wang [3], Laiwei Shen [4], Cheng Huang [4], Jianping Zhu [4], and Wanchun Tang [1,2]

[1] Jiangsu Province Engineering Laboratory of Audio Technology, School of Physics and Technology
Nanjing Normal University, Nanjing, China

[2] Jiangsu Center for Collaborative Innovation in Geographical Information Resource Development and Application
Nanjing, China
eewctang@njnu.edu.cn

[3] College of Electronic and Information Engineering
Nanjing University of Aeronautics and Astronautics, Nanjing, China
jflsjfls@nuaa.edu.cn

[4] School of Electronic and Optical Engineering, Nanjing University of Science and Technology, Nanjing, China
shenlaiwei@yeah.net, hc_win8er@126.com, 169148076@qq.com.

Abstract ─ In this paper, the series-fed dipole array is proposed and studied for near-field radio frequency identification (RFID) applications. The dipole array is composed of several dipoles with a series feed line. Closed form expressions for current distribution and near-field distribution are presented in this paper. To verify the feasibility of this kind of antenna as a reader antenna in near-field ultra-high frequency (UHF) RFID, a prototype that contains three dipoles is designed, fabricated and tested. The theoretic analysis, simulations and experiments agree well and it is shown that the series-fed dipole array is capable of generating strong magnetic field over a rectangular area, which is very useful in near-field UHF RFID applications.

Index Terms ─ Near-field, radio frequency identification, series-fed.

I. INTRODUCTION

Near-field ultra-high frequency (UHF) radio frequency identification (RFID) has become more and more popular for identification and tracking in item level. One of the most common used techniques in near-field UHF RFID is inductive coupling technique for its capability of operating in close proximity to metals and liquids [1, 2].

In general, tags employed in near-field UHF RFID consist of an IC and a loop antenna. To identify such a tag, the magnetic field component that normal to the loop antenna surface should be strong enough [1]. Besides, in some scenarios such as supermarket or library, the goods or books with RFID tags may be distributed at any area of the shelf; hence, the reader antenna is expected to generate a uniform and strong magnetic field over the large rectangular area of the shelf to ensure that every tag can be identified.

There are several strategies to achieve such kind of magnetic field distribution [3-13]. One method is based on zero-phase-shifted (ZPS) line, which is also called segmented line when first proposed in [3]. In this method, capacitors, either lumped [3] or distributed [4, 5], are added to the wire loop to compensate the current phase shift, hence transforming the electrically large antenna to an electrically small antenna and finally enhancing the magnetic field within the antenna area. However, if the antenna is requested to cover a larger area, the design of this kind of antenna will be complicated [6, 7].

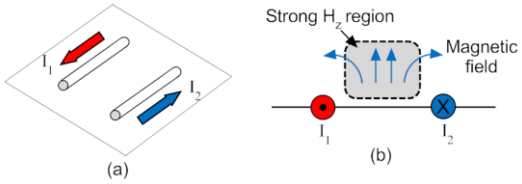

Fig. 1. Schematic of ODCs: (a) perspective view and (b) side view.

Another method is based on the concept of oppositely directed currents (ODCs) [8] shown in Fig. 1, to generate strong magnetic field (referred as strong H_z region here in after) in the area between the two closely spaced currents. To cover a bigger area, a folded dipole antenna is proposed in [9] based on the concept of ODCs, where a 4λ-long loop antenna is folded every half wave length

Submitted On: April 25, 2017
Accepted On: October 19, 2018

to form two "arms" to construct the ODCs. Thanks to its periodic property, this antenna can be extended along the length direction [10, 11] to cover an even longer area.

As can be seen, loop antennas are studied in most of the published literatures for generating strong and uniform magnetic field over a larger area. Less research is reported on the dipole antenna for near-field UHF RFID applications. Inspired by the work of [9], the series-fed dipole array is proposed in this paper, which is composed of several dipoles and a feed line. The dipoles are used to form more than one pair of ODCs, so as to produce strong magnetic field over a larger area for near-field UHF RFID applications. Closed form expressions for the current distributions on the dipoles and near-field magnetic field distributions are presented in this paper. To verify the feasibility of this kind of antenna as a reader antenna in near-field UHF RFID, a prototype that contains three dipoles with series feed line is designed, fabricated and tested. The performance of the prototype is tested by a commercial RFID reader with 30dBm output power and several impinj J41 near-field tags. The prototype occupies an area of 229mm × 126mm, while the measured 100% tag detecting area is bigger than 300mm × 144mm when the observing height is 10mm. The simulations and experiments agree well and it is shown that the series-fed dipole is capable of generating strong magnetic field over a rectangular area, which is very useful in near-field UHF RFID applications.

II. THEORETIC ANALYSIS

Assuming the series-fed dipole array is composed of N dipoles connected in series by a feed line, as shown in Fig. 2. All the N dipoles are made of metal line with radius a, while the lengths l_i (i= 1 to N) of the dipoles and the distances between the adjacent dipoles d_i (i= 1 to N-1) are different and should be optimized. The characteristic admittance of the feed line is denoted as Y_0 with the propagation constant $\beta_0=2\pi/\lambda_g$, where λ_g is the guided wave length of the feed line.

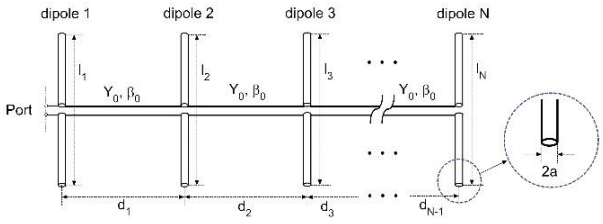

Fig. 2. Configuration of series-fed dipole array.

Before the analysis of this series-fed dipole array, the corresponding equivalent circuit model should be established and shown in Fig. 3, in particular: element circuit model (Fig. 3 (a)) for the N dipoles, feed line circuit model (Fig. 3 (b)), and total equivalent circuit model (Fig. 3 (c)). The analysis of this series-fed dipole will include the currents distribution on the N dipoles and the field distribution of H_z over the antenna area. One should note that the currents on adjacent dipoles should be in opposite direction (or in 180 degree phase difference) in order to form the ODCs. The analysis method is similar to that of log-periodic dipole antenna in [12].

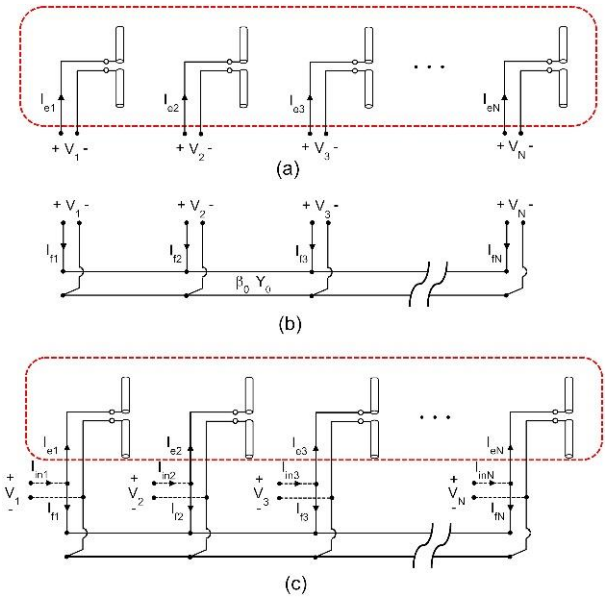

Fig. 3. Equivalent circuit of the series-fed dipole array: (a) element circuit, (b) feed line circuit, and (c) complete circuit.

A. Currents distribution calculation

Considering the element circuit in Fig. 3 (a), the N driving currents of the N dipoles can be represented by $[I_e]$ with the response voltages $[V]$. Let $[Y_e]$ be the admittance matrix of the element circuit, then,

$$[I_e]=[Y_e][V]=[Z_e]^{-1}[V]. \quad (1)$$

The matrix $[Z_e]$ in the above equation is composed of the self- and mutual-impedance of the dipole antenna array, which can be roughly calculated by the formulas in [13, 14] using the induced EMF Method. The formulas are not given here for clarity.

As for the feed line circuit in Fig. 3 (b), similarly, the N driving currents of the N driving ports are represented by $[I_f]$. Since the two circuits (Figs. 3 (a) and (b)) share the same driving ports, the response voltages of the feed line circuit are the same with those of the element circuit, i.e., $[V]$. Let $[Y_f]$ be the admittance matrix of the feed line circuit, we have,

$$[I_f]=[Y_f][V]. \quad (2)$$

$$\left[Y_f\right]=\begin{bmatrix} -jY_0\cot\left(\beta_0 d_1\right) & jY_0\csc\left(\beta_0 d_1\right) & 0 & & 0 \\ jY_0\csc\left(\beta_0 d_1\right) & -jY_0\left[\begin{matrix}\cot\left(\beta_0 d_1\right)\\ +\cot\left(\beta_0 d_2\right)\end{matrix}\right] & jY_0\csc\left(\beta_0 d_2\right) & \cdots & 0 \\ 0 & jY_0\csc\left(\beta_0 d_2\right) & -jY_0\left[\begin{matrix}\cot\left(\beta_0 d_2\right)\\ +\cot\left(\beta_0 d_3\right)\end{matrix}\right] & & 0 \\ & \vdots & & \ddots & \vdots \\ 0 & 0 & 0 & \cdots & -jY_0\cot\left(\beta_0 d_{N-1}\right) \end{bmatrix}. \quad (3)$$

Table 1: Calculated current phase and magnitude of driving currents of the three dipoles

	$\lvert\angle I_2 - \angle I_1\rvert$	$\lvert\angle I_3 - \angle I_2\rvert$	$\lvert I_1\rvert$	$\lvert I_2\rvert$	$\lvert I_3\rvert$
$d_1 = d_2 = 0.4\ \lambda_g$	142.7	261.7	0.76	0.21	0.18
$d_1 = d_2 = 0.5\ \lambda_g$	166.9	166.9	0.34	0.33	0.34
$d_1 = d_2 = 0.6\ \lambda_g$	94.3	205.9	0.92	0.35	0.07

$*\lambda_g$ is assumed to be equal to λ in the calculation, but actually smaller than λ due to the existence of substrates

From the transmission line theory and with the parameters of the feed line (Y_0, β_0 and d_i (i = 1 to N-1)),the matrix $[Y_f]$ can be expressed as equation (3), By connecting the two circuits in Figs. 3 (a) and (b), the input currents at the driving ports shown in Fig. 3 (c) can be obtained by,

$$\left[I_{in}\right]=\left[I_e\right]+\left[I_f\right]=\left(\left[Y_e\right]+\left[Y_f\right]\right)\left[V\right]. \quad (4)$$

Where

$$\left[I_{in}\right]=\left[1 \quad 0 \quad \cdots \quad 0\right]^{-1}. \quad (5)$$

For simplicity, the input current is set equal to 1A.

Substituting equation (1) into equation (4), we have:

$$\left[I_{in}\right]=\left(\left[Y_e\right]+\left[Y_f\right]\right)\left[Z_e\right]\left[I_e\right]. \quad (6)$$

That is,

$$\left[I_{in}\right]=\left(\left[U\right]+\left[Y_f\right]\left[Z_e\right]\right)\left[I_e\right]. \quad (7)$$

where $[U]$ is the unit matrix.

From equation (7), the current distribution $[I_e]$ on the series-fed N dipoles can then be calculated by:

$$\left[I_e\right]=\left[T\right]^{-1}\left[I_{in}\right]. \quad (8)$$

With

$$\left[T\right]=\left[U\right]+\left[Y_f\right]\left[Z_e\right]. \quad (9)$$

As an example, a three-element series-fed dipole array is analyzed. According to the standard UHF RFID in China, 0.92 GHz is selected as the operating frequency, and the lengths of the dipoles are a little shorter than half wavelength (e.g., 0.46λ in this paper) to make the dipole resonant. As to the feed line, typical parameters are used: Y_0 = 1/200 S, $\beta_0 = 2\pi/\lambda_g$ = 19.3 rad/m (λ_g is assumed to be equal to λ).

Using equations (1) – (8), the driving currents of the individual dipole with different d_i (the distance between two adjacent dipoles) are calculated and listed in Table 1. As can be seen, when $d_1 = d_2 = 0.5\lambda_g$, the magnitude of driving currents on the three dipoles are almost the same, and the phase difference of the currents on adjacent dipoles ($|\angle I_2 - \angle I_1|$and $|\angle I_3 - \angle I_2|$) are both equal to 166.9°, near to 180°. As a result, two pairs of ODCs can be formed by the adjacent two dipoles. On the other hand, when $d_1 = d_2 = 0.4\lambda_g$ and $d_1 = d_2 = 0.6\lambda_g$, the current phase difference between the adjacent dipoles do not satisfy the constraints of ODCs, and the current magnitude on the dipole 1 is much bigger than those on other two dipoles. Hence, the distances between two adjacent dipoles are chosen as $d_1 = d_2 = 0.5\lambda_g$.

B. The magnetic field distribution

Once the driving current of each dipole is obtained, the near-field H_z of the array can be roughly calculated by the following equations,

$$H_z\left(x,y,z\right)=\sum_{i=1}^{N}H_{zi}\left(x,y,z\right). \quad (10)$$

Where

$$\mathrm{H}_{zi}\left(x,y,z\right)=-\frac{I_{id}\left(y-y_{0i}\right)}{4\pi r_i^2 j}\left[\begin{matrix} e^{-jkR_{1i}}+e^{-jkR_{2i}} \\ -2\cos\left(\frac{kl}{2}\right)e^{-jkr_i}\end{matrix}\right]. \quad (11)$$

And

$$r_i=\sqrt{((y-y_0 i)^2+(z-z_0 i)^2)}, \quad (12)$$

$$\mathrm{R}_{1i}=\sqrt{\left(x-x_{0i}+l_i/2\right)^2+\mathrm{r}_i^2}, \quad (13)$$

$$R_{2i}=\sqrt{((x-x_0 i-l_i/2)^2+r_i^2)}. \quad (14)$$

where $k=\omega\sqrt{\mu\varepsilon}$. The location of field point is denoted as (x, y, z), while the location at the center of each dipole is represented by (x_{0i}, y_{0i}, z_{0i}) (i = 1 to N). I_{id} (i = 1 to N) is the driving point currents, which can be obtained by equation (8). Here, in this paper, the dipole is assumed very thin and the current distribution along the center-

fed dipole has sinusoidal form [14].

The $|H_z|$ distribution of the three-element series-fed dipole array at different height is then calculated using equation (9) - (10), and the results are plotted in Fig. 4. The three dipoles are all placed on *xoy* plane, and the center point coordinates of the three dipoles are, respectively, (0 mm, 0 mm, 0 mm), (0 mm, 163 mm, 0 mm) and (0 mm, 326 mm, 0 mm).

As can be seen from the Fig. 4, H_z is strong in the area between adjacent dipoles and weak right above the dipoles, just the same as that of the ODCs. When the observing height is 10mm, the $|H_z|$ is relatively strong within the antenna area (0 mm < y < 326 mm) while declines very quickly outside this antenna area. When the observing height h increases, the fluctuation of H_z becomes small and the average $|H_z|$ will decrease. In the region right above the three dipoles, the $|H_z|$ is very small because the magnetic field is in horizontal direction. Such a "weak H_z regions" can be compensated by the same technique in [11].

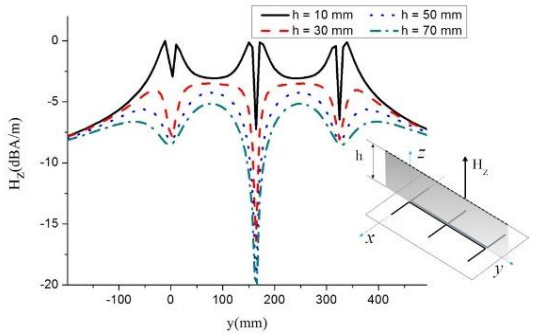

Fig. 4. Calculated $|H_z|$ distribution of the three-element series-fed dipole array f = 0.92 GHz.

III. REALIZATION AND EXPERIMENTS

To verify the performance of the proposed series-fed dipole array, a prototype antenna is design and fabricated. As shown in Fig. 5, the prototype antenna consists of three identical dipoles fed in series by a coplanar stripline (CPS). The antenna is printed on a FR-4 board of 4.4 in dielectric constant and 1.6 mm in thickness. To better match the antenna impedance at the feeding port to 50 Ω, a lumped capacitor is added to the antenna port and taken as 5 pF. Because the prototype antenna is fabricated using standard PCB process, the dimensions of the prototype will be adjusted according to the initial values in section II. Final dimensions of the antenna are: L = 300 mm, W = 144 mm, t = 1.6 mm, L_d = 126 mm, d = 110 mm, w_1 = 3 mm, and w_2 = 2 mm. The current distribution of the antenna at the operating frequency f = 0.92 GHz is obtained by HFSS [15] and shown in Fig. 6. As can be seen, the surface currents I_1 and I_2 are opposite in direction, and the same for I_2 and I_3. This indicates that two pairs of ODCs are formed over the three dipoles.

Figure 7 gives the simulated $|H_z|$ distribution along y-axis of the antenna at observing height of 10mm, 30mm, 50mm and 70mm, respectively. One can see that the simulated magnetic field distribution is similar to that in Fig 4. The "weak H_z regions" occur right above the three dipoles. When the observing height increases ($h \geqslant$ 30 mm), the $|H_z|$ in these three regions decreases quickly and may be smaller than -20dBA/m, the threshold value of $|H_z|$ to identify the tags [8, 13]. Compensation techniques will be employed in the future work to increase the $|H_z|$ above the three dipoles.

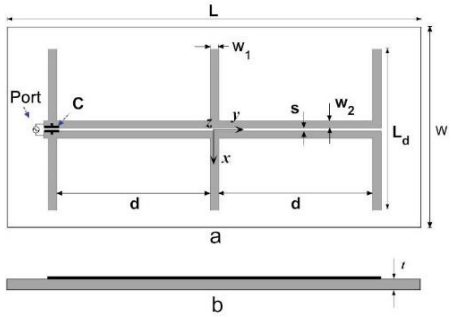

Fig. 5. Geometry of the prototype antenna that contains three elements: (a) top view, and (b) side view.

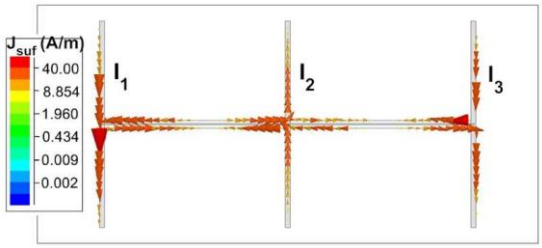

Fig. 6. Simulated current distribution of the prototype antenna.

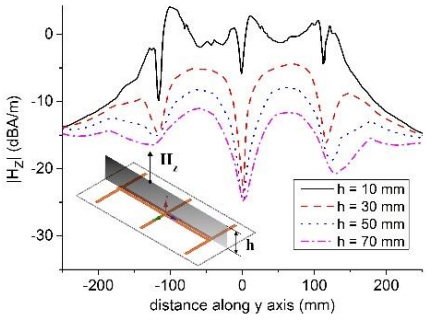

Fig. 7. Simulated $|H_z|$ distribution of the prototype antenna with different observing height (h) at the operating frequency f = 0.92 GHz.

The measured reflection coefficient of the proposed array is given in Fig. 8, together with the simulated results for comparison. One can see that the measured and simulated reflection coefficient agrees well besides a little frequency shift that is caused by the machining accuracy and test environment. As shown in Fig. 8, the measured bandwidth of the array is 0.045 GHz (0.9 GHz – 0.945 GHz) at $|S_{11}| < -10$dB, which can fully satisfy the UHF RFID standard in China.

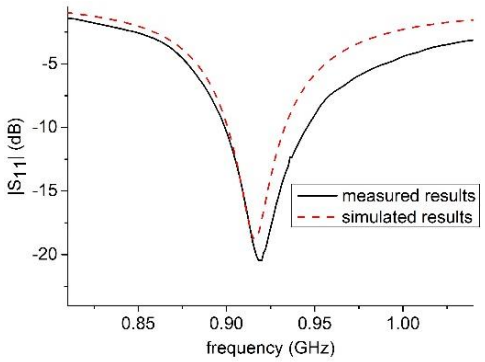

Fig. 8. Simulated and measured $|S_{11}|$ of the prototype antenna.

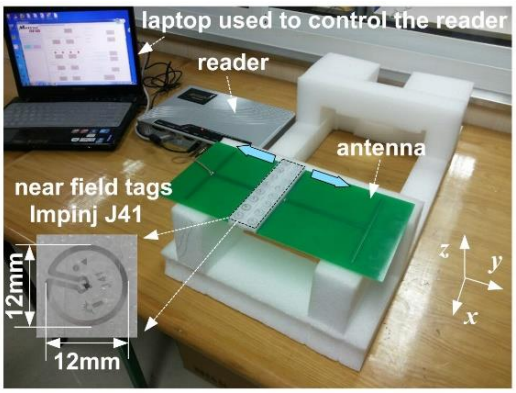

Fig. 9. Experiment setup.

To be used in a real RFID system, the reading performance of the prototype is evaluated using a commercial RFID reader (Marktrace RFID UHF Four Channel Fixed Reader MR6100) and near-field tags (impinj J41). As shown in Fig. 9, the array is connected to the reader by a coaxial-cable, the output power of the reader is set as 30dBm. The tags are placed parallel to the FR-4 board. Figure 10 (a) shows the simulated $|H_z|$ distribution at different observing height, where the area of $|H_z| > -20$ dBA/m is the interrogation area in this paper. The measured interrogation area of the proposed array at different observing height is given in Fig. 10 (b) for comparison. As can be seen, all of the tags are read successfully when the observing height is 10mm with an interrogation area of 300mm × 144mm. When the observing height increases, not all of the tags can be detected and the "weak H_z regions" of $|H_z| < -20$dBA/m will appear. One can see that the "weak H_z regions" in simulated results agree well with those measured results (dark blocks). In the bandwidth of 0.9 GHz to 0.945 GHz, the reading performance of the proposed array is examined and the array works well.

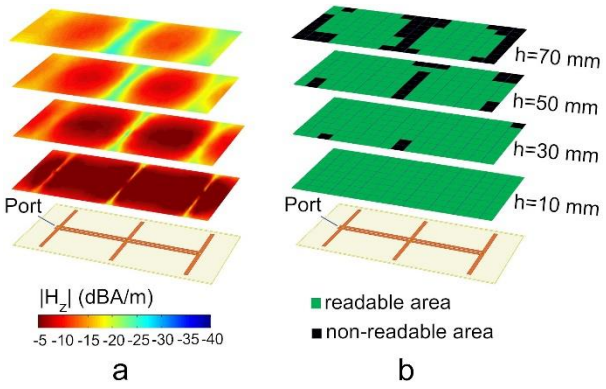

Fig. 10. Simulated $|H_z|$ distribution and measured reading area of the prototype antenna at different observing height: (a) simulated $|H_z|$ distribution, and (b) measured reading area of the proposed array.

IV. CONCLUSION

In this paper, the series-fed dipole array is proposed and studied for near-field UHF RFID application. The method of calculating the current distribution and the near-field distribution of the series-fed array is presented. A prototype that contains three dipoles is designed, fabricated and measured. The simulations and experiments agree well and it is proved that the series-fed dipole is capable of generating a strong magnetic over a rectangular area, which is very useful in near-field UHF RFID applications.

ACKNOWLEDGMENT

This work is supported by the National Key Research and Development Program of China (Grant No. 2017YFB0503500) and the National Natural Science Foundation of China (Grant No. 61571232).

REFERENCES

[1] P. V. Nikitin, K. V. S. Rao, and S. Lazar, "An overview of near field UHF RFID," *Proc. IEEE Int. Conf. RFID*, Grapevine, pp. 167-174, 2007.

[2] A. R. Partridge. "Accuracy in action: Item-level RFID takes off," *Apparel Magazine*, 2013.

[3] D. M. Dobkin, S. M. Weigand, and N. Iye, "Segmented magnetic antennas for near-field UHF RFID," *Microwave Journal*, vol. 56, no. 6, pp. 872-873, 2007.

[4] X. Qing, Z. Chen, J. Shi, and C. K. Goh, "Zero-phase-shift line antennas," *International Workshop on Antenna Technology (iWAT)*, pp. 179-182, 2013.
[5] X. Qing, C. K. Goh, and Z. Chen, "A broadband UHF near-field RFID antenna," *IEEE Transaction on Antennas and Propagation*, vol. 58, no. 12, pp. 3829-3838, 2010.
[6] J. Shi, X. Qing, and Z. N. Chen, "Electrically large zero-phase-shift line grid-array UHF near-field RFID reader antenna," *IEEE Trans. Antenna Propag.*, vol. 62, no. 4, pp. 2201-2207, 2014.
[7] A. Sharma, I. J. G. Zuazola, J. C. Batchelor, et al., "Dual purpose near- and far-field UHF RFID coil antenna with non-uniformly distributed-turns," *IEEE Antennas & Wireless Propagation Letters*, vol. 14, pp. 1342-1345, 2015.
[8] C. Cho, J. Ryoo, I. Park, and H.Choo, "Design of a novel ultra-high frequency radio-frequency identification reader antenna for near-field communications using oppositely directed currents," *IET Microw. Antennas Propag.*, vol. 4, pp. 1543-1548, 2010.
[9] D. Xumin, W. Qun, Z. Kuang, and F. Chunnan, "A magnetic coupling dipole for UHF near-field RFID reader," *IEEE Trans. Magn.*, vol. 48, no. 11, pp. 4305-4308, 2012.
[10] L. Shen, W. Tang, H. Xiang, and W. Zhuang, "A novel antenna achieving null-less magnetic field distribution for near-field UHF RFID," *Antennas and Propagation (ISAP), 2014 International Symposium on*, Kaohsiung, pp. 547-548, 2014.
[11] L. Shen, W. Zhuang, W. Tang, and J. Ma, "Achieving uniform perpendicular magnetic field distribution for near-field UHF RFID," *IET Microw. Antennas Propag.*, vol. 10, no. 2, pp. 215-222, 2016.
[12] R. Duhamel and D. Isbell, "Broadband logarithmmically periodic antenna structures," *Ire International Convention Record IEEE*, pp. 119-128, 1966.
[13] H. E. King, "Mutual impedance of unequal length antennas in echelon," *IEEE Trans. Antennas Propag.*, vol. AP-5, pp. 306-313, 1957.
[14] C. A. Balanis, *Integral Equations, Moment Method, and Self and Mutual Impedances, in Antenna Theory: Analysis and Design*, 3rd ed., New Jersey: John Wiley & Sons, pp. 461-473, 2005.
[15] ANSYS High Frequency Structure Simulator, http://www.ansys.com/

Yi Wang (M' 15) received the B.S. and Ph.D. degrees in Communication and Information System from Nanjing University of Aeronautics and Astronautics (NUAA), Nanjing, China, in 2006 and 2012. In 2012, he joined the College of Electronic and Information Engineering, NUAA, as an Assistant Professor. Currently he is working there as an Associate Professor. His research interests include computational electromagnetics, and the earthquake electromagnetics.

Laiwei Shen was born in Anhui Province, China, in 1990. He received the B.S. degree from Nanjing University of Science and Technology in 2011. Currently, he received the Ph.D. degree From Nanjing University of Science and Technology in 2017. His research interests include RF/microwave circuit, and modeling and optimization of RFIC, antennas.

Cheng Huang was born in Jiangsu Province, China, in 1989. He received the B.S. degree from Nanjing University of Science and Technology, Nanjing, China in 2011. Currently, he is working towards the Ph.D. degree at Nanjing University of Science and Technology. His current research interests include RF/microwave circuit, and modeling and optimization of RFIC, antennas.

Jianping Zhu was born in Anhui Province, China, in 1986. He received the B.S. degree from Anhui University, Hefei, in School of Electronics and Information Engineering in 2010. Currently, he is working towards the Ph.D. degree at Nanjing University of Science and Technology. His current research interests include RF/microwave circuit, through silicon via and frequency-selective surfaces.

Wanchun Tang (M'04) was born in China in 1967. He received the B.S. degree from Tsinghua University, Beijing, China, in 1990, the M.S. degree from the Nanjing University of Science and Technology (NJUST), Nanjing, China, in 1995, and the Ph.D. degree from the City University of Hong Kong, Hong Kong, in 2003, all in electrical engineering.

He was a Full Professor with the Department of Communication Engineering, NJUST, and is currently a Specially Invited Full Professor with the Jiangsu Ley Laboratory on Optoelectronic Technology, School of Physics and Technology, Nanjing Normal University, Nanjing. He has authored or coauthored over 100 journal and conference papers. His current research interests include modeling and optimization of RFIC antennas, signal integrity, and power integrity design in package.